PROCEEDINGS A

royalsocietypublishing.org/journal/rspa

Research

Cite this article: Amendola A, Mattei O, Milton GW, Seppecher P. 2023 The obstacle problem in no-tension structures and cable nets. *Proc. R. Soc. A* **479**: 20220229. https://doi.org/10.1098/rspa.2022.0229

Received: 1 April 2022
Accepted: 29 November 2022

Subject Areas:
civil engineering, computational mathematics, structural engineering

Keywords:
force networks, truss structures, no-tension response, limit analysis

Author for correspondence:
Graeme W. Milton
e-mail: graeme.milton@utah.edu

The obstacle problem in no-tension structures and cable nets

Ada Amendola[1], Ornella Mattei[2], Graeme W. Milton[3] and Pierre Seppecher[4]

[1]Department of Civil Engineering, University of Salerno, Fisciano, Salerno, Italy
[2]Department of Mathematics, San Francisco State University, San Francisco, CA, USA
[3]Department of Mathematics, University of Utah, Salt Lake City, UT, USA
[4]Institut de Mathématiques de Toulon, Université de Toulon et du Var, France

AA, 0000-0002-2562-881X

We consider the problem of finding a net that supports prescribed point forces, yet avoids certain obstacles, with all the elements of the net being under compression (or all being under tension), and being confined within a suitable bounding box. In the case of masonry structures, when described through the simple, no-tension constitutive model, this consists, for instance, in finding a strut net that supports the forces, is contained within the physical structure, and avoids regions that may be not accessible. We solve such a problem in the two-dimensional case, where the prescribed forces are applied at the vertices of a convex polygon, and we treat the cases of both single and multiple obstacles. By approximating the obstacles by polygonal regions, the task reduces to identifying the feasible domain in a linear programming problem. For a single obstacle we show how the region Γ available to the obstacle can be enlarged as much as possible in the sense that there is no other strut net, having a region Γ' available to the obstacle with $\Gamma \subset \Gamma'$. The case where some of the forces are reactive is also treated.

Electronic supplementary material is available online at https://doi.org/10.6084/m9.figshare.c.6350216.

THE ROYAL SOCIETY PUBLISHING

1. Introduction

The mechanical modelling of masonry structures is a rather complex task, due to the heterogeneous nature of the material, its ordered or disordered subdivision in blocks and mortar beds, and the peculiar sensitivity of masonry to fracture damage (see, e.g. [1–3] and references therein). A simple model introduced by Heyman [4] describes the masonry as a compression-only (or no-tension) homogeneous material, which exhibits infinite compression strength and is not affected by failure modes due to the relative sliding between the blocks [4]. Such a model does not account for shear failure, which is nevertheless of paramount importance in different cases of technical interest [2,3]. It can be safely applied when rocking-type failure is expected to anticipate shear failure [3]. According to Heyman's model, a well-known 'master safe' theorem states that the collapse of a masonry arch does not occur if a line of thrust of the given external loads can be fit within the boundaries of the arch (see [4] and also [5–7]). The line of thrust coincides with Hooke's inverted chain of the given forces, as shown, e.g. by the Italian engineer Poleni in a study dated back to 1784, which was aimed at assessing the stability of St. Peter's dome in the Vatican [8]. Such a construction has been the foundation of the beautiful work of the Catalan architect Antoni Gaudí on funicular shapes of masonry structures [9,10]. An interesting numerical procedure to construct the thrust line of a masonry arch that is closest to the axis line is given in [11], while the influence of settlements on the load-bearing capacity of masonry arches and different masonry structures is studied in [12]. The use of truss networks within discrete element approaches to no-compression or no-tension bodies is frequent in the literature (refer to [13–17] and references therein). Truss models are convenient, e.g. to tackle the equilibrium problem of masonry structures, described as no-tension bodies [18,19], and to assess the compatibility of external loads through graphical constructions, numerical methods and hanging models [15–17,20–22]. Polyhedral Airy stress functions have been employed in two-dimensional problems, since such functions permit one to conveniently describe force networks through scalar potentials [23,24]. It is worth remarking that the no-tension model does not account for buckling analysis, since the material is supposed to behave rigidly up to collapse, and not to fail in shear [4,25].

A recent study has investigated the existence problem of systems of tensile forces that support given sets of nodal forces, coming to the conclusion that if such 'cable webs' exist then the given forces are supported by the complete web connecting pairwise their points of application (see [13], theorem 1.1). In two dimensions, and with forces at the vertices of a convex polygon, the use of polyhedral Airy stress functions shows alternatively that if such 'cable webs' exist then the given forces can be supported by an open web with no internal loops (see [14], theorem 1, and figure 1).

The present work generalizes the above problem to the case of compression-only force networks (or 'strut nets') in two dimensions, which support given sets of nodal forces, and are able to avoid 'obstacles' representing regions not accessible to the force network (e.g. holes or inclusions). We begin by deriving a result showing that a strut net supporting q forces located strictly inside the convex hull of the points where forces are applied and avoiding p obstacles can be replaced by a strut net with at most $p+q$ elementary loops (§2). From then onwards we restrict our attention to sets of forces at the vertices of a convex polygon ($q=0$). In §3, we provide a condition for the non-existence of strut nets that avoid a given obstacle, when such an obstacle intersects the open strut net associated with the given forces, and extends outside the convex hull of their points of application. We also provide an algorithm to establish if there exists a strut net avoiding multiple obstacles, and if so to construct one. Additionally, for a single obstacle, we show how the region available to the obstacle can be enlarged as much as possible (in a sense to be made more precise). Section 4 treats the case of multiple obstacles with the inclusion of reactive forces. Numerical applications are then presented in §5, by first dealing with a test problem characterized by a single active force, and then by treating a series of examples that analyse strut nets associated with the statics of masonry arches. We end in §6 by drawing concluding remarks and directions for future work.

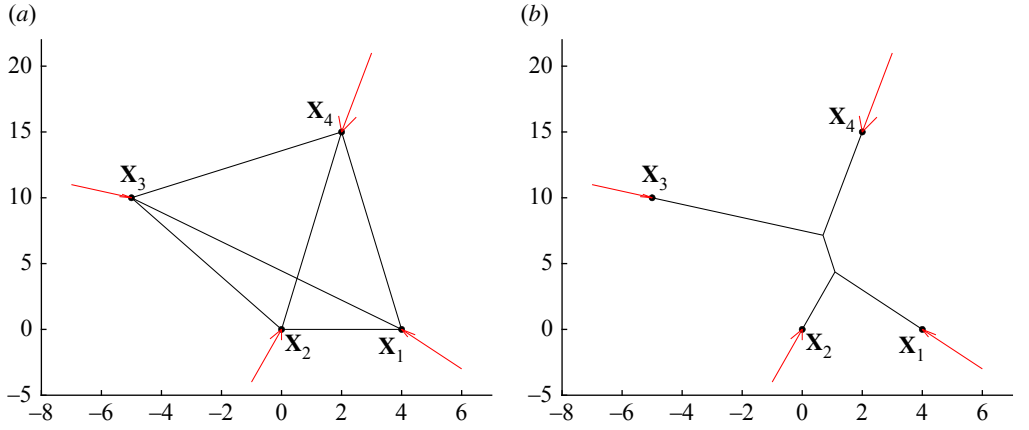

Figure 1. As proved in [13], a strut net that supports forces applied at the vertices of a convex polygon, such as the forces depicted in red in (*a*), is the one connecting pairwise their points of application. Such a strut net, represented in black, is not the only one. For example there always exists an open net, shown in (*b*), that supports such a set of forces with no internal loops.

2. Reducing the complexity of a strut net avoiding a given set of obstacles

To begin, we consider a set of points $\mathbf{x}_1, \mathbf{x}_2, \ldots, \mathbf{x}_n$ at the vertices of a convex polygon Ω, with external forces $\mathbf{t}_1, \mathbf{t}_2, \ldots, \mathbf{t}_n$ acting on them. We assume that the points are numbered anticlockwise and we adopt the following convention: for any $i > n$, $\mathbf{x}_i := \mathbf{x}_{i-n}$ and $\mathbf{x}_0 := \mathbf{x}_n$. Letting

$$\mathbf{R}_\perp = \begin{pmatrix} 0 & -1 \\ 1 & 0 \end{pmatrix}$$

denote the matrix for a 90° rotation, we assume that, for all j with $1 \le j \le n$ and for all i with $j \le i \le j + n - 1$,

$$\sum_{k=j}^{i} (\mathbf{x}_k - \mathbf{x}_j) \cdot [\mathbf{R}_\perp \mathbf{t}_k] \ge 0. \tag{2.1}$$

This assumption ensures that there exists a truss structure supporting these forces with all the struts in the truss structure under compression [14]. The constraint (2.1) has a physical interpretation: the net anticlockwise torque around the point $\mathbf{x}_j$ of the forces $\mathbf{t}_k$ summed over any number of consecutive points clockwise past the point $\mathbf{x}_j$ is non-positive. If (2.1) is satisfied, the forces are supported by an open strut net with no internal loops, in other words, there are no polygons whose edges are the struts of the net. A more general condition, applicable to any set of forces, either in two dimensions or three dimensions, is that if a strut net exists supporting the forces, then they will also be supported by a strut net connecting pairwise the points at which the forces are applied [13]. This leads to a linear programming problem for determining if a set of forces can be supported.

Condition (2.1) is derived using Airy stress functions. Indeed, for two-dimensional elasticity it is well known that, in the absence of body forces in a simply-connected region Ω, the divergence-free stress field $\boldsymbol{\sigma}(\mathbf{x})$ can be represented in terms of the Airy stress function $\phi(\mathbf{x})$:

$$\boldsymbol{\sigma}(\mathbf{x}) = \begin{pmatrix} \dfrac{\partial^2 \phi(\mathbf{x})}{\partial^2 x_2^2} & -\dfrac{\partial^2 \phi(\mathbf{x})}{\partial x_1 \partial x_2} \\ -\dfrac{\partial^2 \phi(\mathbf{x})}{\partial x_1 \partial x_2} & \dfrac{\partial^2 \phi(\mathbf{x})}{\partial^2 x_1^2} \end{pmatrix} = \mathbf{R}_\perp^T \nabla\nabla\phi(\mathbf{x}) \mathbf{R}_\perp, \tag{2.2}$$

in which $\mathbf{R}_\perp^T = -\mathbf{R}_\perp$ is the transpose of $\mathbf{R}_\perp$. Since $\boldsymbol{\sigma}(\mathbf{x})$ is negative semidefinite for all $\mathbf{x}$, we see that $\nabla\nabla\phi(\mathbf{x})$ is negative semidefinite for all $\mathbf{x}$. This implies that $\phi(\mathbf{x})$ is a concave function in any simply-connected two-dimensional region under compression, that may have subregions with zero stress [18]. Note that, when $\boldsymbol{\sigma}(\mathbf{x})$ is zero in a region, as it is between the struts in a net, then $\nabla\nabla\phi(\mathbf{x}) = 0$ which by (2.2) implies the Airy stress function is a linear function of $\mathbf{x}$ in this region. Thus, any strut net under compression that supports forces at the vertices of a convex polygon will have an associated Airy stress function whose graph is a concave polyhedron. The magnitudes of the slope discontinuities can be connected to the compression in the associated struts [24,26].

If the strut net associated with a concave polyhedron has internal loops, we can replace the latter by a simpler concave polyhedron (supporting the same forces), by using the tangent planes to the Airy stress function at the boundary of the polygon Ω [14]. The strut net associated with this latter concave polyhedron will be an open strut net with no internal loops. To prove this, let us start by noticing that, since the strut net supports under compression the forces $\mathbf{t}_i$ at the points $\mathbf{x}_i$, it can support, for some $\epsilon > 0$, the same forces at points

$$\tilde{\mathbf{x}}_i = \mathbf{x}_i - \epsilon \mathbf{t}_i, \tag{2.3}$$

the convex hull of which we call $\tilde{\Omega}$. To do this, one extends the strut net by attaching n short struts of length $\epsilon > 0$ between $\mathbf{x}_i$ and $\tilde{\mathbf{x}}_i$, $i = 1, 2, \ldots, n$. The first step is to determine the Airy stress function $\phi(\mathbf{x})$ in the polygonal ring bounded on one side by the polygon joining the points $\mathbf{x}_i$, and on the other side by the polygon joining the points $\tilde{\mathbf{x}}_i$. When ϵ is sufficiently small there are no struts inside the quadrilateral Ω_i with vertices $\tilde{\mathbf{x}}_{i-1}$, $\mathbf{x}_{i-1}$, $\mathbf{x}_i$, $\tilde{\mathbf{x}}_i$ and since the stress vanishes there, the Airy stress function $\phi(\mathbf{x})$ inside that quadrilateral must be a linear function $L_i(\mathbf{x})$. Due to the stress in the wires (see, for example, [14]), these satisfy

$$\mathbf{R}_\perp(\nabla L_{i+1} - \nabla L_i) = -\mathbf{t}_i, \quad i = 1, 2, \ldots, n, \tag{2.4}$$

and, for all i, j,

$$L_i \geq L_j \quad \text{on } \Omega_j. \tag{2.5}$$

Equation (2.4) and the constraints

$$L_i(\mathbf{x}_i) = L_{i+1}(\mathbf{x}_i) \tag{2.6}$$

determine the sequence $(L_i)_{i=1}^n$ up to the addition of a global linear function. Uniqueness can be ensured by assuming, for instance, that $L_1(\mathbf{x}) = 0$. The condition (2.5) is equivalent to (2.1) [14].

The stress measure $\boldsymbol{\sigma}(\mathbf{x})$ associated with the Airy function $\phi(\mathbf{x})$, that is defined in the sense of distributions by (2.2), is non-positive, concentrated along a finite union of segments, divergence-free on Ω and, owing to the construction of $(L_i)_{i=1}^n$, the divergence in the sense of distributions, $\mathrm{div}(\sigma_{|\Omega})$, coincides with the discrete measure $\sum_{i=1}^n \mathbf{t}_i \delta_{\mathbf{x}_i}$ on $\partial\Omega$. Let us introduce the following definition:

Definition 2.1. A 'strut net function' is a concave piecewise linear function $\phi(\mathbf{x})$ on $\widetilde{\Omega}$ coinciding with $L_i(\mathbf{x})$ on each Ω_i.

We see that, in particular, the envelope of the tangent planes,

$$\phi_0(\mathbf{x}) \equiv \min_i L_i(\mathbf{x}), \tag{2.7}$$

is a strut net function: we call it the 'open strut net function' as it is associated with a strut net having no loops. Note also that concavity implies that any strut net function $\phi(\mathbf{x})$ satisfies, for all i, $\phi(\mathbf{x}) \leq L_i(\mathbf{x})$, and hence that $\phi(\mathbf{x}) \leq \phi_0(\mathbf{x})$.

(a) Forces at points inside the convex hull of all application points and multiple obstacles

Consider a strut net containing a convex elementary polygonal loop within which there are no obstacles. By elementary we mean a loop with no interior struts. Then, the net forces (due to adjoining struts or imposed forces) act on the vertices of the loop as in figure 2*a*, and the polygonal loop can be replaced by an open strut net, as in figure 2*b*. In this way, if there are

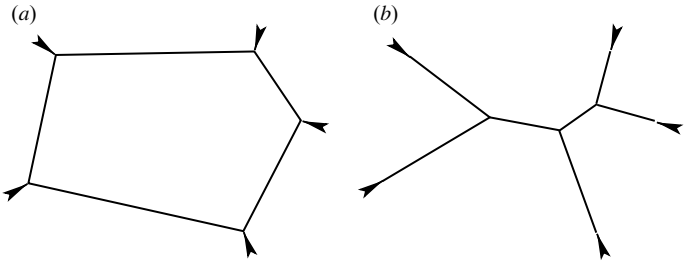

Figure 2. Here (*a*) is a convex polygonal loop, possibly lying within a strut net that may contain many loops. The arrows denote the net forces acting on each vertex. Provided there are no obstacles inside the loop, it can be replaced by the open strut net as in (*b*), thus reducing the number of loops in the whole strut net by one.

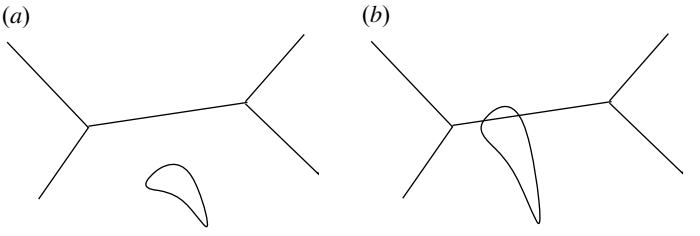

Figure 3. An obstacle may lie partly outside the convex hull of where the forces are applied, but outside the open strut net, as in (*a*). However, if the obstacle lies partly outside the convex hull of where the forces are applied and intersects the open strut net, as in (*b*), then there is no strut net that avoids the obstacle.

many internal loops in the strut net, we decrease the number of elementary loops by one. This reduction can be continued until any remaining elementary loop encloses one or more obstacles or has an imposed force acting outwards from a vertex of the polygonal loop, so that the loop is not convex.

Then, using the fact that any obstacle intersecting the boundary of the convex hull of all points where forces are applied can never have a loop of struts under compression surrounding it, we establish:

Theorem 2.2. *A strut net that has q imposed forces at points that lie strictly inside the convex hull of all points where forces are applied and that avoids p obstacles, p_0 of which intersect the boundary of this convex hull, can be replaced by a strut net, supporting the same forces, that has at most $q + p - p_0$ elementary loops.*

This generalizes the result in [13] that used a similar argument to treat the case where $p = p_0 = 0$ ($q \neq 0$).

If a loop contains an obstacle it may be possible to replace that loop by the associated open strut net provided that open strut net does not collide with the obstacle. In the $q = 0$ case it follows that, if a net exists that avoids a single obstacle, then there is a net with none or one loop that also avoids the obstacle. Specifically, the zero loop case corresponds to the open strut net, and if there is one loop that cannot be reduced, then that loop contains the obstacle. Note that, as the struts in the loop are under compression, the loop cannot extend outside the convex hull of the points where the forces are applied. Thus, if an obstacle intersects the open strut net and extends outside the convex hull of the points where the forces are applied, then there is no strut net that avoids the obstacle (see figure 3).

3. Solution for the obstacle problem with forces at the boundary of a convex polygon

Our objective is to find an algorithm for determining if a strut net exists that avoids a given set of simply connected obstacles and which supports a given set of forces at the boundary of a convex polygon. We will first assume that there is just one obstacle and we will enlarge the region it can occupy. Here by enlargement we use the following definitions:

Definition 3.1. Given a strut net avoiding an obstacle $\mathcal{O}$, the region Γ available to $\mathcal{O}$ is the interior of the strut loop, having no internal struts, that contains $\mathcal{O}$.

Definition 3.2. Given a region Γ available to $\mathcal{O}$ for some strut net, then Γ' is an enlargement of it if Γ' is available to $\mathcal{O}$ for some strut net and $\Gamma' \supseteq \Gamma$.

Thus, if the obstacle is in a region Γ, then it is surely in the enlarged region Γ': $\mathcal{O} \subseteq \Gamma$ implies $\mathcal{O} \subseteq \Gamma'$. While the procedure will be illustrated by figures in which there are only four applied forces, the analysis holds when there are any number of forces applied at the vertices of a convex polygon.

Given a strut net, and associated strut net function $\psi(\mathbf{x})$, we can modify the strut net to try to accommodate, or better accommodate, an obstacle $\mathcal{O}$ by replacing $\psi(\mathbf{x})$ with

$$\phi(\mathbf{x}) = \min\{\psi, L\}, \quad \text{with } L(\mathbf{x}_k) \geq L_k(\mathbf{x}_k) \quad \text{for all } k, \tag{3.1}$$

where $L(\mathbf{x})$ is a linear function to be chosen so that $\phi(\mathbf{x}) = L(\mathbf{x})$ on $\mathcal{O}$. Thus, $\psi(\mathbf{x}) \geq L(\mathbf{x})$ on $\mathcal{O}$. We call $L(\mathbf{x})$ the cleaving plane. Now, if for any $\mathbf{x}$,

$$L(\mathbf{x}) \leq \psi(\mathbf{x}), \tag{3.2}$$

then surely because $\psi(\mathbf{x}) \leq \phi_0(\mathbf{x})$, one has that

$$L(\mathbf{x}) \leq \phi_0(\mathbf{x}). \tag{3.3}$$

Thus, the region Γ available to the obstacle is enlarged if the cleaving plane cleaves the open strut net function rather than any other strut net function supporting the forces (see figure 4*a–d*).

Hence, the existence of a strut net avoiding the obstacle $\mathcal{O}$ is equivalent to the existence of a linear function $L(\mathbf{x})$ satisfying

$$L(\mathbf{x}_i) \geq L_i(\mathbf{x}_i) \quad \text{and} \quad L(\mathbf{x}) \leq L_i(\mathbf{x}) \quad \text{on } \mathcal{O} \text{ for all } i. \tag{3.4}$$

(a) One or more obstacles which are convex polygons, or which can be approximated by convex polygons

Note that, for any cleaving plane $L(\mathbf{x})$, the set $\{\mathbf{x} : \phi_0(\mathbf{x}) \geq L(\mathbf{x})\}$ is a convex set because of the concavity of the open strut net function $\phi_0(\mathbf{x})$. Hence, there is no loss of generality by assuming that the obstacle $\mathcal{O}$ is convex. Therefore, consider the case when the obstacle $\mathcal{O}$ is a convex polygon or is approximated by a convex polygon containing the obstacle $\mathcal{O}$. Let $\mathbf{y}_p, p = 1, 2, \ldots, m$ be the vertices of this polygon. Then, (3.4) will hold if $L(\mathbf{x})$ satisfies

$$L(\mathbf{x}_i) \geq a_i \equiv \phi_0(\mathbf{x}_i) \quad \text{and} \quad L(\mathbf{y}_p) \leq b_p \equiv \phi_0(\mathbf{y}_p) \quad \text{for all } i, p. \tag{3.5}$$

Now, $L(\mathbf{x})$ can be written as $L(\mathbf{x}) = \mathbf{v} \cdot \mathbf{x} + c$ and we are looking for $\mathbf{v}$ and c so that the inequalities (3.5) are satisfied, that is, for all i and p,

$$\mathbf{v} \cdot \mathbf{x}_i + c \geq a_i \quad \text{and} \quad \mathbf{v} \cdot \mathbf{y}_p + c \leq b_p. \tag{3.6}$$

The question becomes whether there is a feasible domain of $(\mathbf{v}, c)$ pairs satisfying this system of linear inequalities: this is a standard problem in linear programming theory.

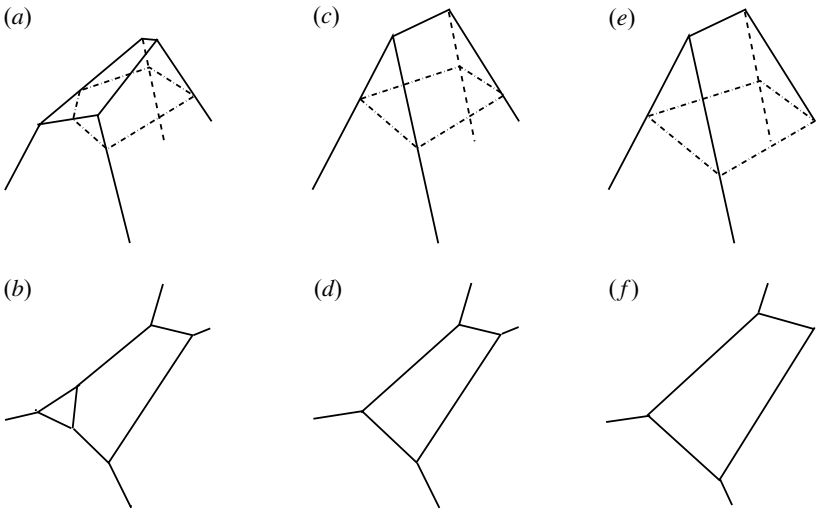

Figure 4. Here (*a*) shows the cleaving (dot-dash line) of a strut net function (solid and dashed lines), resulting in the strut net (*b*). If instead as in (*c*) one cleaves, with the same cleaving plane, the open strut net function, one enlarges the region that the obstacle can occupy, and the corresponding strut net (*d*) has a single elementary internal loop. Finally, by moving the cleaving plane downwards keeping the same orientation until it touches one of points $L_k(\mathbf{x}_k)$, as in (*e*), one further enlarges the region that the obstacle can occupy, as in (*f*).

Note that this is easily generalized to the case of multiple inclusions $\mathcal{O}_q,\ q=1,2,\ldots,s$, with associated cleaving planes $L^{(q)}(\mathbf{x})$. Then, (3.4) is replaced with

$$L^{(q)} \geq L_i(\mathbf{x}_i) \quad \text{and} \quad L^{(q)} \leq L_i, \quad L^{(q)} \leq L^{(r)} \text{ on } \mathcal{O}_q, \text{ for all } i,q,r. \tag{3.7}$$

Treating each inclusion $\mathcal{O}_q$ as convex or approximating it by a convex polygon containing $\mathcal{O}_q$, we let $\mathbf{y}_p^{(q)}, p=1,2,\ldots,m(q)$ be its vertices. Then (3.7) will hold if the cleaving planes $L^{(q)}(\mathbf{x})$ satisfy for all i,p,r

$$L^{(q)}(\mathbf{x}_i) \geq a_i \equiv \phi_0(\mathbf{x}_i) = L_i(\mathbf{x}_i), \tag{3.8}$$

and

$$L^{(q)}(\mathbf{y}_p^{(q)}) \leq b_p^{(q)} \equiv \phi_0(\mathbf{y}_p^{(q)}) \quad \text{and} \quad L^{(q)}(\mathbf{y}_p^{(q)}) \leq L^{(r)}(\mathbf{y}_p^{(q)}). \tag{3.9}$$

Writing $L^{(q)}(\mathbf{x})$ as $L^{(q)}(\mathbf{x}) = \mathbf{v}^{(q)} \cdot \mathbf{x} + c^{(q)}$ we arrive at the linear system of inequalities

$$\left.\begin{aligned} &\mathbf{v}^{(q)} \cdot \mathbf{x}_i + c^{(q)} \geq a_i, \quad \mathbf{v}^{(q)} \cdot \mathbf{y}_p^{(q)} + c^{(q)} \leq b_p^{(q)} \\ \text{and} \quad &\mathbf{v}^{(r)} \cdot \mathbf{y}_p^{(q)} + c^{(r)} - \mathbf{v}^{(q)} \cdot \mathbf{y}_p^{(q)} + c^{(q)} \geq 0, \end{aligned}\right\} \tag{3.10}$$

which must hold for all i,q and r. This is again a standard problem of determining if there is a non-empty feasible domain in the $3s$ dimensional space consisting of s pairs $(\mathbf{v}^{(q)}, c^{(q)})\ q=1,2,\ldots,s$. If it is non-empty, then associated with a $(\mathbf{v}^{(q)}, c^{(q)})\ q=1,2,\ldots,s$ in the feasible domain are cleaving planes $L^{(q)}(\mathbf{x}),\ q=1,2,\ldots,s$ and when $\phi_0(\mathbf{x})$ is cleaved by them we obtain the strut net avoiding the obstacles.

(b) Enlarging as much as possible the region available to the obstacle

Let us return to the case where there is a single obstacle and assume that the feasible domain associated with (3.6) is non-empty. While the feasible domain allows us to identify all strut nets with one strut loop that contains the obstacle $\mathcal{O}$, it does not identify those strut nets with as much room as possible around the obstacle $\mathcal{O}$. By this we mean that the region Γ available to the obstacle $\mathcal{O}$ is maximal, in the sense that if Γ' is the region available to the obstacle $\mathcal{O}$ in another

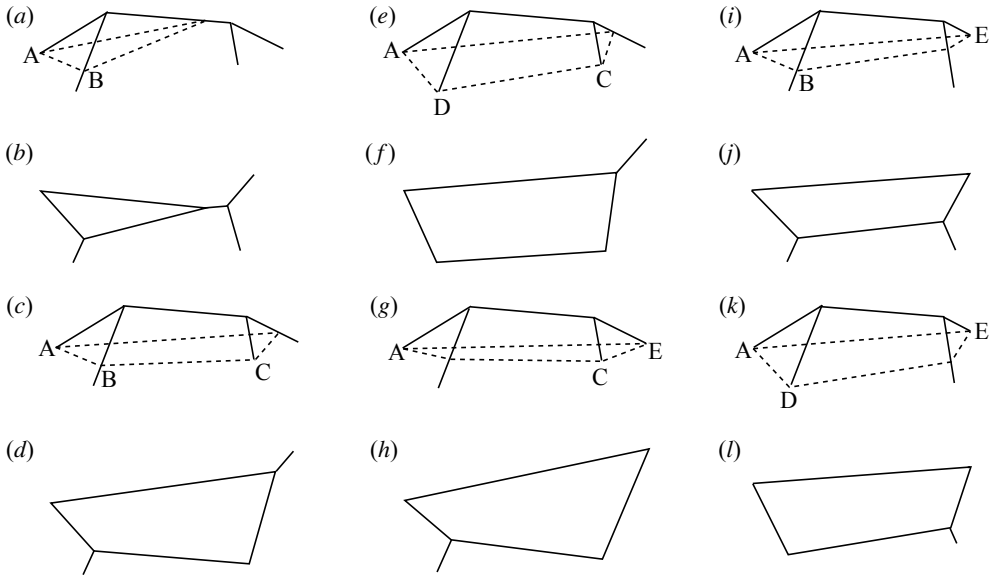

Figure 5. Various configurations, (*a*), (*c*), (*e*), (*g*,*i*) and (*k*) of the cleaving plane, denoted by dashed lines, that cleave $\phi_0(\mathbf{x})$, denoted by solid lines. The associated strut nets are below each of these subfigures. The procedure of tilting and then rotating the cleaving plane follows that described in the text.

strut net and $\Gamma \subseteq \Gamma'$, then $\Gamma' = \Gamma$. Note that Γ is not necessarily unique, and a different Γ may have less room around the obstacle on one side and more on another side. Here, we will show that if the obstacle $\mathcal{O}$ lies in a maximal Γ then

$$L(\mathbf{x}_k) = L_k(\mathbf{x}_k) \quad \text{and} \quad L(\mathbf{x}_\ell) = L_\ell(\mathbf{x}_\ell), \tag{3.11}$$

for some k and ℓ.

If, for any $\mathbf{x}$, (3.3) holds then surely

$$L'(\mathbf{x}) \le \phi_0(\mathbf{x}) \quad \text{with } L' = L - \min_i (L(\mathbf{x}_i) - a_i), \quad a_i = L_i(\mathbf{x}_i), \tag{3.12}$$

because $L'(\mathbf{x}) \le L(\mathbf{x})$. In other words, the cleaving plane can be lowered while keeping its orientation fixed, expanding the region Γ that can be occupied by the obstacle. This can be continued until this cleaving plane L' first touches a point $A = L_k(\mathbf{x}_k)$, where $i = k$ attains the equality in (3.12) (see figure 3).

Now we tilt the cleaving plane about the line through A and another point $B \in L \cap L_k$ with $B \neq A$. This line is where $L'(\mathbf{x})$ and $L_k(\mathbf{x})$ intersect. This gives a new cleaving plane

$$L'' = L' + \alpha(L' - L_k), \quad \text{with } \alpha > 0. \tag{3.13}$$

We can continue this tilting by increasing α until

$$\alpha = \min_j \frac{L'(\mathbf{x}_j) - L_j(\mathbf{x}_j)}{L_k(\mathbf{x}_j) - L'(\mathbf{x}_j)}, \tag{3.14}$$

when $L''(\mathbf{x})$ first touches another point $C = L_\ell(\mathbf{x}_\ell)$ in which $j = \ell$ achieves the equality in (3.14). It also touches A. Note that if for any $\mathbf{x}$ the first inequality in (3.12) holds then surely

$$L''(\mathbf{x}) \le \phi_0(\mathbf{x}), \tag{3.15}$$

because that first inequality implies $L'(\mathbf{x}) \le L_k(\mathbf{x})$ at that point. This implies that as the cleaving plane is tilted until it touches B, the region Γ that can be occupied by the obstacle enlarges further (see figure 5*a*–*d*).

One can subsequently rotate the cleaving plane about the line joining A with $L_\ell(\mathbf{x}_\ell)$ until the cleaving plane meets $L_h(\mathbf{x}_h)$ for some h. In our example, rotation one way gives figure 5*e* with $L_h(\mathbf{x}_h) = D$ and the corresponding strut net figure 5*f*, while rotation the other way gives figure 5*g* with $L_h(\mathbf{x}_h) = E$ and the corresponding strut net figure 5*h*. However, this rotation does not generally enlarge the region Γ that can be occupied by the obstacle. The rotation tips the cleaving plane up on one side of the line $L_k(\mathbf{x}_k)$ with $L_\ell(\mathbf{x}_\ell)$ and down on the other side. The region Γ, with the strut loop as its boundary, shrinks on the up side and expands on the down side. The exception, as illustrated in figure 5*i* with the corresponding strut net figure 5*j* is when $\ell = k \pm 1$, i.e. when $L_\ell(\mathbf{x}_\ell)$ is on the same facet of $\phi_0(\mathbf{x})$ as $L_k(\mathbf{x}_k)$. Then the region Γ lies on one side of the line joining $\mathbf{x}_k$ with $\mathbf{x}_\ell$ and, as illustrated in figure 5*k* we may rotate the cleaving plane about the line so the plane tilts down on the side where Γ is located and touches $D = L_h(\mathbf{x}_h)$, producing the strut net of figure 5*l*.

This analysis provides an algorithm to generate all maximal regions Γ. One starts with each $i = 1, 2, \ldots, n$ and takes the cleaving plane through $L_i(\mathbf{x}_i)$, $L_{i+1}(\mathbf{x}_{i+1})$ and a third point $L_j(\mathbf{x}_j)$ (with no points $L_h(\mathbf{x}_h)$, $h = 1, 2, \ldots, n$ lying above the plane). One next rolls the cleaving plane, rotating it about the line joining $L_i(\mathbf{x}_i)$ and $L_j(\mathbf{x}_j)$ until it first hits another point $L_k(\mathbf{x}_k)$. Then one rolls it further about the line joining $L_i(\mathbf{x}_i)$ and $L_k(\mathbf{x}_k)$ until it first hits another point $L_\ell(\mathbf{x}_k)$. This is continued until the rolling cleaving plane hits $L_{i-1}(\mathbf{x}_{i-1})$. As the rolling progresses the region enclosed by the strut net loop created by the cleaving plane is maximal and the region available to an obstacle placed within it cannot be enlarged.

4. Including reactive forces with multiple obstacles

Let us suppose that a subset $\mathcal{I} \subset \{1, \ldots, n\}$ of the n forces are reactive, while the remaining ones (corresponding to the subset of indices $\mathcal{K} := \{1, \ldots, n\} \setminus \mathcal{I}$) are given. That means that the forces are not fixed at the points $\mathbf{x}_i$ for $i \in \mathcal{I}$ but that any forces at these points are admissible as soon as they balance through a strut net the forces $\mathbf{t}_i$ applied at points $\mathbf{x}_i$ for $i \in \mathcal{K}$. The planes L_k are no longer fixed by equations (2.4). When $i \in \mathcal{I}$, these equations determine the reactive force $\mathbf{t}_i$:

$$\mathbf{t}_i \equiv -\mathbf{R}_\perp(\nabla L_{i+1} - \nabla L_i), \quad i \in \mathcal{I} \tag{4.1}$$

and provide no constraints on the unknown L_{i+1} and L_i while, for the remaining $i \in \mathcal{K}$, they provide the constraints

$$\mathbf{R}_\perp(\nabla L_{i+1} - \nabla L_i) = -\mathbf{t}_i, \quad i \in \mathcal{K}. \tag{4.2}$$

Since we can add any linear function to the Airy stress function, we are free to assume, as before, that

$$L_1 = 0. \tag{4.3}$$

Continuity of the Airy function requires that, for all $i \in \{1, 2, \ldots, n\}$,

$$L_{i+1}(\mathbf{x}_i) = L_i(\mathbf{x}_i). \tag{4.4}$$

Its concavity requires that, for all $i \neq j$ in $\{1, 2, \ldots, n\}$,

$$L_j(\mathbf{x}_i) \geq L_i(\mathbf{x}_i). \tag{4.5}$$

As in (3.10), the existence of a strut net avoiding the s obstacles $\mathcal{O}_1$, $\mathcal{O}_2$, …, $\mathcal{O}_s$, each $\mathcal{O}_q$ being the convex hull of points $(\mathbf{y}_1^q, \mathbf{y}_2^q, \ldots, \mathbf{y}_{n(q)}^q)$, is equivalent to the existence, for all $q \in \{0, 1, \ldots, s\}$, of linear functions $L^{(1)}$, $L^{(2)}$, …, $L^{(s)}$ satisfying, for any i in $\{0, 1, \ldots, n\}$, any $q \neq r$ in $\{0, 1, \ldots, s\}$ and any p in $\{0, 1, \ldots, n(q)\}$,

$$L^{(q)}(\mathbf{x}_i) \geq L_i(\mathbf{x}_i), \quad L_i(\mathbf{y}_p^{(q)}) \geq L^{(q)}(\mathbf{y}_p^{(q)}) \quad \text{and} \quad L^{(r)}(\mathbf{y}_p^{(q)}) \geq L^{(q)}(\mathbf{y}_p^{(q)}). \tag{4.6}$$

These results, which also generalize the results obtained in §3, can be summarized in the following theorem:

Theorem 4.1. *The existence of a strut net balancing forces $\mathbf{t}_i$ applied at points $(\boldsymbol{x}_i)_{i\in\mathcal{K}}$ with the help of reacting points $(\boldsymbol{x}_i)_{i\in\mathcal{I}}$ and avoiding obstacles $\mathcal{O}_1$, $\mathcal{O}_2$, …, $\mathcal{O}_s$, each $\mathcal{O}_q$ being the convex hull of points $(\boldsymbol{y}_1^q, \boldsymbol{y}_2^q, \ldots, \boldsymbol{y}_{n(q)}^q)$, is equivalent to the existence of linear functions $(L_i)_{i=1}^n$ and $(L^{(q)})_{q=1}^s$ satisfying, for any i in $\{0,1,\ldots,n\}$, any $q\neq r$ in $\{0,1,\ldots,s\}$ and any p in $\{0,1,\ldots,n(q)\}$, the constraints (4.2)–(4.6). Setting*

$$L_i(\boldsymbol{x}) = \boldsymbol{w}_i\cdot\boldsymbol{x} + d_i \quad \text{and} \quad L^{(q)}(\boldsymbol{x}) = \boldsymbol{v}^{(q)}\cdot\boldsymbol{x} + c^{(q)}, \tag{4.7}$$

the existence of such a strut net is equivalent to the existence of a solution $(\boldsymbol{w}_i, d_i)_{i=1}^n$ and $(\boldsymbol{v}^{(q)}, c^{(q)})_{q=1}^s$ of the following linear programming problem

$$\left.\begin{aligned}
&\boldsymbol{R}_\perp(\boldsymbol{w}_{i+1}-\boldsymbol{w}_i) = -\boldsymbol{t}_i, \quad \text{for } i\in\mathcal{K},\\
&\boldsymbol{w}_1 = 0, \quad d_1 = 0,\\
&\boldsymbol{w}_{i+1}\cdot\boldsymbol{x}_i + d_{i+1} = \boldsymbol{w}_i\cdot\boldsymbol{x}_i + d_i, \quad \text{for } 1\le i\le n,\\
&\boldsymbol{w}_j\cdot\boldsymbol{x}_i + d_j \ge \boldsymbol{w}_i\cdot\boldsymbol{x}_i + d_i, \quad \text{for } i\neq j \text{ in } \{1,\ldots,n\},\\
&\boldsymbol{v}^{(q)}\cdot\boldsymbol{x}_i + c^{(q)} \ge \boldsymbol{w}_i\cdot\boldsymbol{x}_i + d_i, \quad \text{for } 1\le i\le n, 1\le q\le s,\\
&\boldsymbol{w}_i\cdot\boldsymbol{y}_p^{(q)} + d_i \ge \boldsymbol{v}^{(q)}\cdot\boldsymbol{y}_p^{(q)} + c^{(q)}, \quad \text{for } 1\le i\le n, 1\le q\le s, 1\le p\le n(q)\\
\text{and}\quad &\boldsymbol{v}^{(r)}\cdot\boldsymbol{y}_p^{(q)} + c^{(r)} \ge \boldsymbol{v}^{(q)}\cdot\boldsymbol{y}_p^{(q)} + c^{(q)}, \quad \text{for } q\neq r \text{ in } \{1,\ldots,s\}, 1\le p\le n(q).
\end{aligned}\right\} \tag{4.8}$$

Recall that, as soon as admissible quantities $(\mathbf{w}_i, d_i)_{i=1}^n$ have been chosen, the reacting forces are determined by (4.1).

We must emphasize the fact that, when a solution exists for the previous linear programming problem, generally an infinity of solutions exists. Indeed we have not fixed any objective function to minimize. We can fix in very different ways such a linear objective function. But even when it is given uniqueness is not guaranteed. This fact is clearly illustrated by the following example. Assume that all bars in the strut net have a thickness proportional to the force they carry, in such a way that the stress remains constant in the whole structure. Then the total volume $\mathcal{V}$ of the structure is proportional to the integral over Ω of the Laplacian of the strut net function (a negative measure). This linear function of the unknowns, which from here onwards we will call the total weight of the structure, seems to be a good candidate for the objective function. However, one can note that, using the divergence theorem, $\mathcal{V}$ can be computed from the normal derivative of the strut net function on the boundary of the domain. Therefore, it does not involve the $L^{(q)}$ functions: its minimization can help fix the L_i functions, that is the reactive forces, but it cannot entirely determine a unique strut net.

We can also treat the case when a subset $\mathcal{J}\subseteq\mathcal{I}$ of the points at which the reactive forces act, rather than being fixed, are confined to some line segments. These segments, for example, could be sections of supporting walls or ground. Then, there are the constraints

$$\mathbf{x}_j\cdot(\mathbf{R}_\perp\mathbf{g}_j) = z_j \quad \text{and} \quad g_j^- \le \mathbf{x}_j\cdot\mathbf{g}_j \le g_j^+, \quad \text{for } j\in\mathcal{J}, \tag{4.9}$$

where the unit vectors $\mathbf{g}_j$ and constants z_j, g_j^- and g_j^+ are given, but only defined for $j\in\mathcal{J}$. These segments should be such that the $\mathbf{x}_i, i=1,2,\ldots,n$ are still the vertices, going anticlockwise, of a convex polygon for all choices of points $\mathbf{x}_j, j\in\mathcal{J}$ anywhere on the line segments. Now we need to add the $\mathbf{x}_j, j\in\mathcal{J}$ to the unknowns. Then, those equations in (4.8) that involve $\mathbf{x}_j, j\in\mathcal{J}$ provide quadratic (and non-convex) constraints on the unknowns, and we are left with determining the feasible domain associated with a quadratic programming problem, involving (4.8) and (4.9), again a standard problem.

It could be the case that reactive forces act at, say, a pair of neighbouring points $\mathbf{x}_i$ and $\mathbf{x}_{i+1}$ with $i\in\mathcal{J}$ and $i+1\in\mathcal{J}$ and share the same line segment. Then,

$$\mathbf{g}_i = \mathbf{g}_{i+1}, \quad z_i = z_{i+1}, \quad g_i^- = g_{i+1}^- \quad \text{and} \quad g_i^+ = g_{i+1}^+, \tag{4.10}$$

and to maintain the anticlockwise order of points (4.9) needs to be electronic supplementary material, supplemented by the additional constraint that

$$(\mathbf{x}_i - \mathbf{x}_{i+1}) \cdot \mathbf{g}_i \geq 0, \tag{4.11}$$

by, if necessary, reversing the direction of $\mathbf{g}_i$, the signs of z_i, g_i^- and g_i^+, and reversing the inequalities in (4.9), while maintaining (4.10). The generalization to the case of more reactive forces acting at neighbouring points sharing the same interval is straightforward.

There is an alternative to allowing the points $\mathbf{x}_j, j \in \mathcal{J}$ to range along these line segments: one can distribute along each line segments sufficiently many additional fixed points $\mathbf{x}_i$ at which reactive forces act. This has the advantage of replacing the quadratic programming problem with a linear one, generally at the sacrifice of having more unknowns. This is what has been done in the numerical examples in §5c where 200 points with reactive forces have been distributed along two supporting segments.

5. Numerical results

The first part of this section deals with some numerical applications of theorem 2.2 of §2, the second part treats the issue of enlarging the region where the obstacle can be placed, while the last part discusses numerical examples of the linear programming procedure described in theorem 4.1 of §4. Specifically, in §5a, we consider two examples in which the internal loops of a strut net that avoids an obstacle are simplified into open strut nets, up to a certain number of irreducible elementary loops. Indeed, according to theorem 2.2 in §2, the number of loops that cannot further be simplified depends on the number of points of application of the forces that lie inside the convex hull and on the position of these forces and the obstacle itself. In §5b, we implement the algorithm, presented at the end of §3, that allows one to enlarge the area available to place an obstacle. Finally, in §5c, strut nets are generated that support sets of active applied forces at given points and reactive forces at other given points that act in response to the applied forces. The first example gives a strut net with two triangular cells that supports a single active force and avoids four obstacles. Four subsequent examples examine strut net models for masonry arches modelled as rigid no-tension bodies [4,17], which are subject to different loading conditions and are required to avoid various obstacles. In all the examples of sections from §5a to 5c(i), we use abstract units for lengths and forces. We omit the indication of such units for ease of notation. The final examples of §5c(ii) deal with a real case of a masonry structure described through the no-tension model. Such examples analyse the triumphal arch of a basilica church studied in [27], both in correspondence of the real configuration of the structure, and also in correspondence of a modified configuration that exhibits additional holes/obstacles applied to the side abutments. We wish to remark that all the results given in the previous sections are scale invariant. Indeed, historically the stability of masonry arches was assessed by building scaled models and testing their stability (see, e.g, [10]). The numerical results presented hereafter are illustrative examples of the algorithm given in section §4, which works also for more complicated problems.

(a) Loop reduction

(i) Reduction to a funicular arch strut net

Let us consider strut net models of a semicircular masonry arch with horizontal span of the extrados equal to 18, a rise at the intrados of 7.6 and a thickness of 1.4 (in abstract units, see figure 6 for a graphical illustration of the current example). The arch is loaded by a set of nine active forces with unit magnitude directed downwards, uniformly distributed at equal angles of $\pi/20$ along the extrados, and two reactive forces acting at the ends of the arch. Reactive forces in equilibrium with the assigned active loads, and an initial strut net featuring $\ell = 13$ closed loops were obtained by employing the numerical procedure presented in [28] (a unique material was assigned to all the struts, cf. figure 6*a*). Such a strut net was next reduced to an open strut net ($\ell = 0$), employing

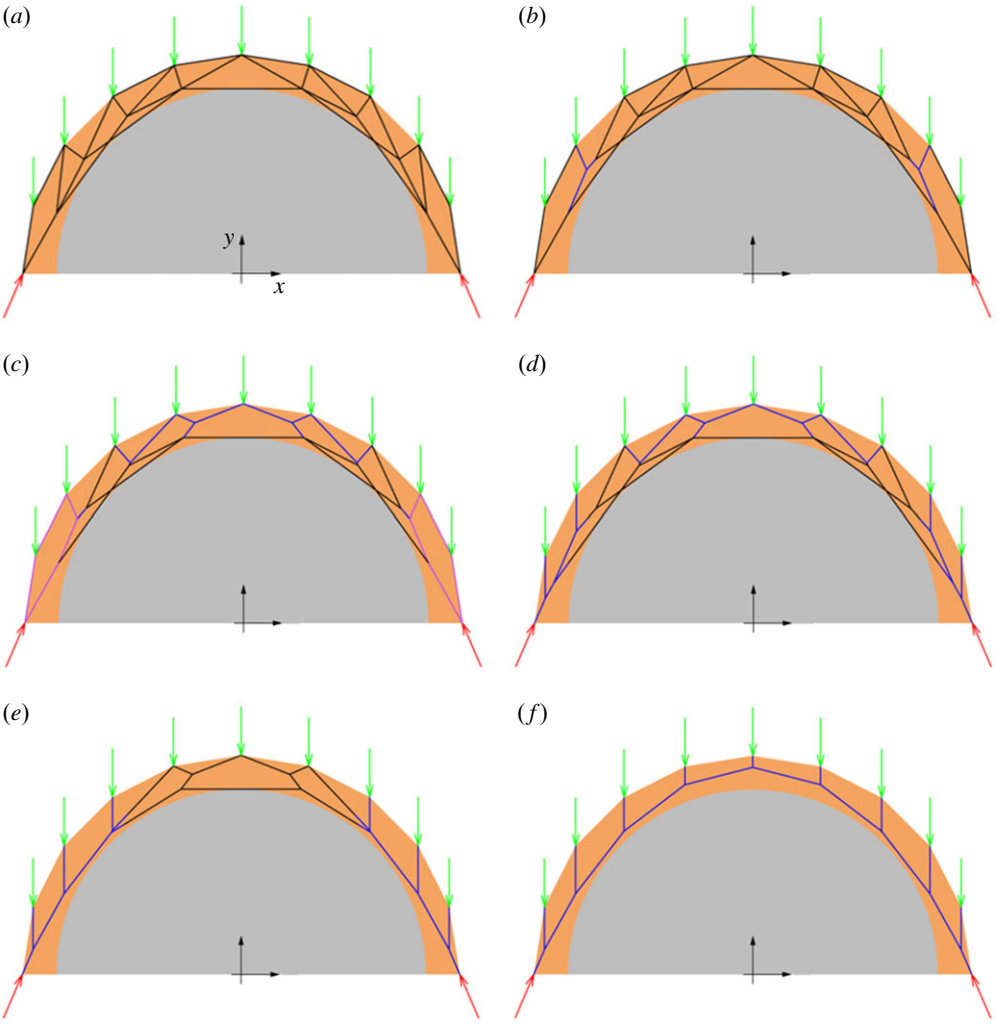

Figure 6. Simplification of an arched strut net that supports nine vertical forces (in green) of equal magnitude acting downwards along the extrados of the masonry arch, here represented in orange, with the help of two supporting reactive forces (marked in red) acting at the endpoints of the arch. In order for the strut net to be contained in the masonry structure, it has to avoid the half disk represented in grey. (*a*) The initial strut net exhibiting $\ell = 13$ closed loops. In (*b–f*), the loop reduction procedure presented in [13] is applied to reduce each closed loop so that the final strut net is an open net, as shown in (*f*). In each panel the open net replacing a closed loop is highlighted in a shade of purple. Note that the reactive forces at the endpoints of the arch have been scaled by a factor of 0.2. See also movie S1 in the electronic supplementary material.

the loop reduction procedure presented in [13] (see figure 6*b–e* and electronic supplementary material, movie S1). Since the active and reactive external forces of the current example are applied at the vertices of a convex polygon ($q = 0$), it is easily observed that $\ell \leq q + p - p_0$, in agreement with theorem 2.2 of §2. It is easy to show that the open strut net coincides with the funicular polygon of the active forces, which passes through the endpoints of the arch and has the initial and final segments parallel to the lines of the reactive forces [29] (see also [11]). Note that the open strut net function $\phi_0(\mathbf{x})$ for this example, plotted in figure 7*a* for $L_1 = 0$, provides the open strut net in figure 7*b*, which coincides with the one represented in figure 6*f*, obtained through loop reduction.

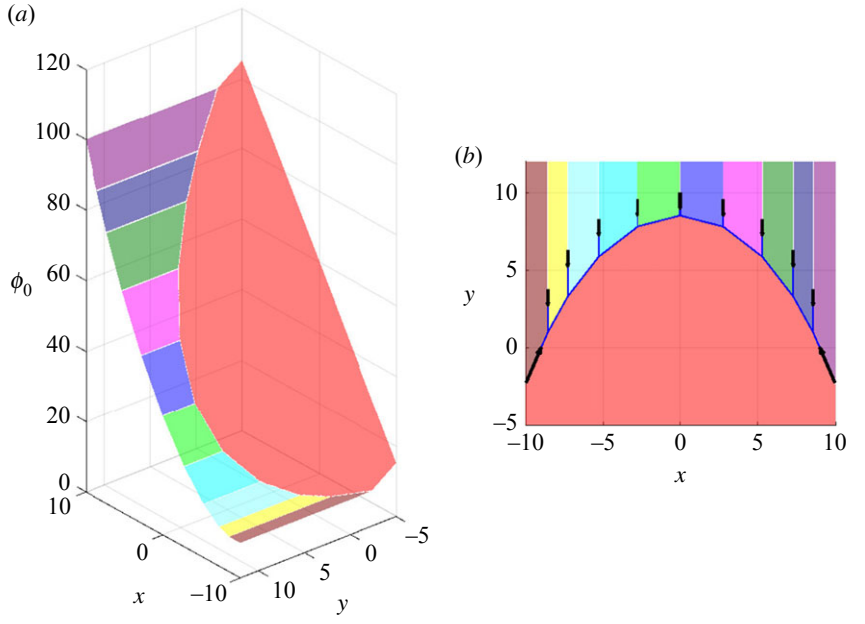

Figure 7. (*a*) Here is the open strut net function $\phi_0(\mathbf{x})$, defined in (2.7), associated with the example considered in figure 6. By definition, $\phi_0(\mathbf{x})$ is the envelope of the tangent planes $L_i(\mathbf{x})$ (here $i = 1, \ldots, 11$), represented by the 11 coloured regions in the picture. Here, $L_1 = 0$. The intersection between the 11 planes provides the associated open strut net, as shown in (*b*). As expected, the latter coincides with the one depicted in figure 6*f*, obtained via loop reduction. Note that the reactive forces at the endpoints of the arch have been scaled by a factor of 0.5.

(ii) Loop reduction for a strut net with an internal force and that avoids an obstacle

Here, we consider the example depicted in figure 8*a*, in which one of the forces, $\mathbf{f}_4 = (0.874, 0.574)$, is applied inside the polygon formed by the remaining forces. Indeed, the point $\mathbf{x}_4 = (5, 5)$, lies inside the polygon formed by $\mathbf{x}_1 = (10, 0)$, $\mathbf{x}_2 = (0, 0)$, $\mathbf{x}_3 = (-5, 10)$ and $\mathbf{x}_5 = (12, 7)$ where the forces $\mathbf{f}_1 = (2.751, -2.319)$, $\mathbf{f}_2 = (-3.415, -1.933)$, $\mathbf{f}_3 = (-3.149, 1.786)$ and $\mathbf{f}_5 = (2.938, 1.891)$ are applied. According to the theory presented in [13], a strut net supporting such forces with all the elements under compression exists. An example is provided by the strut net connecting all the points pairwise as showed in figure 8*a*. Now suppose that an obstacle is placed inside one of the loops of the strut net. As stated by theorem 2.2 in §2, in which $q = 1$, $p = 1$ and $p_0 = 0$, we can replace the strut net connecting the points pairwise by one that has at most $q + p - p_0 = 2$ elementary loops, as shown in electronic supplementary material, movie S2. The result of the loop reduction is portrayed in figure 8*b*, where the two remaining elementary loops cannot be reduced further.

(b) Enlarging the region available to the obstacle

In this section, we provide a numerical example that illustrates the algorithm presented at the end of §3 to enlarge the region available to the obstacle. We start with seven forces, $\mathbf{f}_1 = (-1, -4)$, $\mathbf{f}_2 = (-3, -1)$, $\mathbf{f}_3 = (-2, 2)$, $\mathbf{f}_4 = (-3, 5)$, $\mathbf{f}_5 = (1, 1)$, $\mathbf{f}_6 = (6, 2)$ and $\mathbf{f}_7 = (2, -5)$, applied, respectively, at the points $\mathbf{x}_1 = (0, 0)$, $\mathbf{x}_2 = (-16, 7)$, $\mathbf{x}_3 = (-13, 16)$, $\mathbf{x}_4 = (2, 20)$, $\mathbf{x}_5 = (12, 19)$, $\mathbf{x}_6 = (12, 13)$ and $\mathbf{x}_7 = (10, 0)$ of the Cartesian frame illustrated in figure 9. The open strut net function for this example is shown in figure 9*a*, and the associated open strut net is represented in figure 9*b*. In order to find the maximal regions Γ, we start with point $\mathbf{x}_1$ and consider the cleaving plane passing through $L_1(\mathbf{x}_1)$, $L_2(\mathbf{x}_2)$ and $L_3(\mathbf{x}_3)$, see figure 9*c*, which provides the region Γ depicted in black in figure 9*d*. Then, we roll the cleaving plane about the line connecting $L_1(\mathbf{x}_1)$ and $L_3(\mathbf{x}_3)$, until the plane touches the point $L_4(\mathbf{x}_4)$, figure 9*e*,*f*, and this is continued until the plane touches $L_7(\mathbf{x}_7)$, as showed in

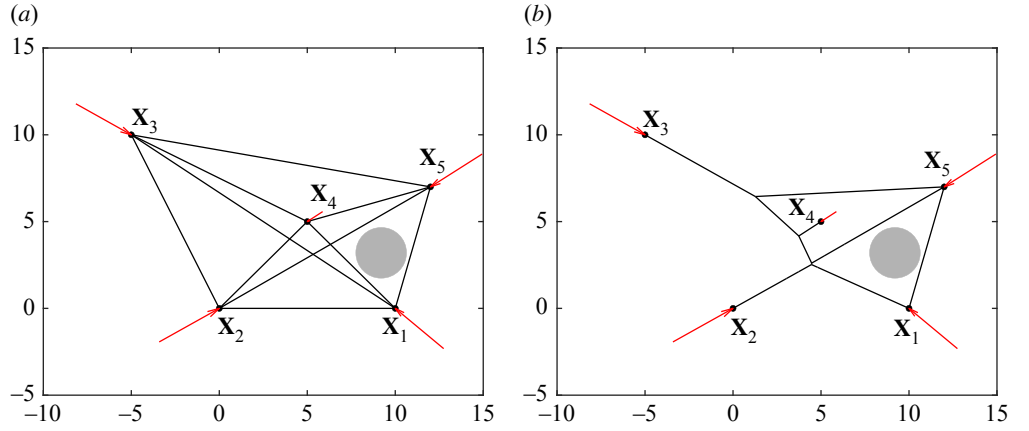

Figure 8. (*a*) A strut net, in black, that supports the applied forces, in red, and avoids the obstacle (here represented by the grey circle) is the one connecting the points pairwise. By applying loop reduction, as illustrated step-by-step in movie S2 in the electronic supplementary material, it is possible to reduce the number of elementary loops with at most $q + p - p_0 = 2$ remaining loops, as illustrated in (*b*). Note that the two remaining loops cannot be simplified further due to the presence of the obstacle, on the one hand, and the force applied at the point x_4, which lies inside the convex hull of the forces, on the other hand.

figure 9*g*,*h*. Movie S3 in the electronic supplementary material shows the rolling of the plane from the initial configuration figure 9*c* to the final configuration figure 9*h*: as the rolling occurs, the region in which the obstacle can be placed is maximal.

(c) Construction of strut nets avoiding obstacles

(i) A strut net avoiding triangular and square inclusions

Let us search for a strut net that supports a single active vertical force (pointing downward) applied to the point with coordinates (0, 4), with respect to the Cartesian frame illustrated in figure 10. We examine two supporting segments delimited by the points (−4, 0) and (3, 4) (segment 1) and the points (3, 0) and (4, 0) (segment 2), which are placed on the opposite extremities of the strut net. Each of such segments is composed of 100 fixed reaction points uniformly spaced along the span of the segment. The searched strut net needs to avoid four obstacles, which are formed by three triangles ($T1$, $T2$ and $T3$) and one rectangle (R). The coordinates of the vertices of such polygons are defined as follows

— $T1$ [(1, 2); (3, 2); (3, 3)]; $T2$ [(0, 1.3); (0.2, 3.5); (−0.2, 3.5)]; $T3$ [(−2.5, 0.5); (−1, 0.5); (−1, 2)];
— R [(−2, 1.2); (−2, 3); (−3, 3); (−3, 1.2)].

Figure 10 illustrates four strut nets obtained through the linear programming algorithm of §4 using different objective functions. The result in figure 10*a* was obtained by minimizing the total weight of the structure, i.e. the integral over the boundary of the domain of the normal derivative of the strut net function. In this case, the optimal strut net is composed of seven struts and two elementary loops. The strut nets in figure 10*b–d* were instead obtained by minimizing the heights of the cleaving planes of the obstacles $T1$, $T2$ and $T3$ at their centres of mass, respectively. By minimizing one of such functions, the goal is to enlarge the room available to the corresponding obstacle. It does not always achieve this goal because the minimization can tilt the cleaving plane, or move the surrounding facets of the Airy stress function. The strut net in figure 10*b* is again composed of seven struts and two elementary loops, as that in figure 10*a*. The strut net in figure 10*c* is instead formed by five struts and one loop, while that in figure 10*d* shows ten struts

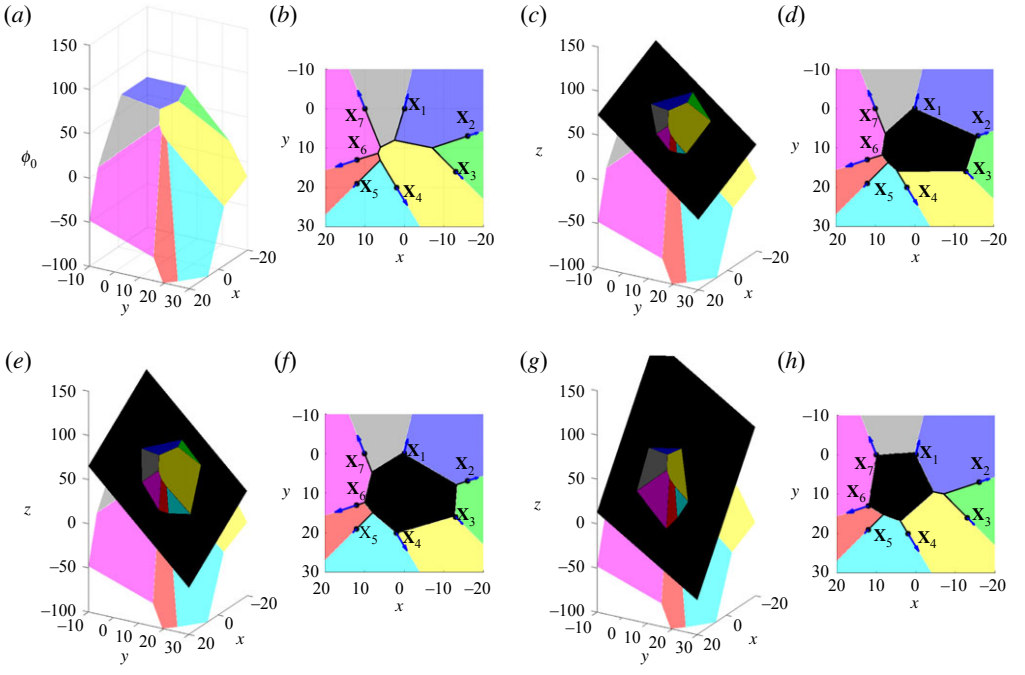

Figure 9. (*a*) The open strut net function $\phi_0(\mathbf{x})$, which by its definition, given by equation (2.7), represents the envelope of the tangent planes $L_i(\mathbf{x})$ (here $i = 1, \ldots, 7$), represented by the seven coloured regions in the picture. Here, $L_1 = 0$. The intersection between the seven planes provides the associated open strut net, as shown in (*b*). In (*c*), a cleaving plane (represented in black) passing through the points $L_1(\mathbf{x}_1)$, $L_2(\mathbf{x}_2)$ and $L_3(\mathbf{x}_3)$, intersects $\phi_0(\mathbf{x})$ to create a region displayed in black in (*d*) where an obstacle can be placed. Indeed, one can replace the open strut net in (*b*) with a strut net containing a loop represented by the sides of the black polygon in (*d*) and place an obstacle in such a loop. We roll, then, the cleaving plane about the line connecting $L_1(\mathbf{x}_1)$ and $L_3(\mathbf{x}_3)$, until the plane touches the point $L_4(\mathbf{x}_4)$, see (*e*). The rolling of the cleaving plane will identify a new strut net with a closed loop represented by the side of the black region in (*f*) where one can place an obstacle. At this point, we let the plane roll about the line connecting $L_1(\mathbf{x}_1)$ and $L_4(\mathbf{x}_4)$, until it reaches the point $L_6(\mathbf{x}_6)$. Lastly, we let the cleaving plane roll about the line connecting $L_1(\mathbf{x}_1)$ and $L_6(\mathbf{x}_6)$ until it touches $L_7(\mathbf{x}_7)$, as shown in (*g*). The corresponding strut net with a closed loop is represented in (*h*). The rolling of the plane is illustrated step by step in movie S3 in the electronic supplementary material. Note that, by applying this procedure to the remaining points $\mathbf{x}_i$, $i = 2, \ldots, 7$, we can find the maximal feasible areas that an obstacle can occupy.

and two loops. Observe that in most directions more space is available to obstacle 3 in figure 10*c* rather than figure 10*d*. Solutions like those in figure 10*c*, where there are no struts separating two obstacles, can be enforced, if possible, by treating the two obstacles as a single obstacle.

(ii) Arched strut nets avoiding openings and inclusions

The concluding examples that we examine in the present study deal with the real case of a masonry structure modelled through the no-tension approach by Heyman. We analyse the triumphal arch of the San Ippolisto Martire basilica church (Atripalda, Italy, 1584–1612), which was previously studied in [27] through a finite element approach. The triumphal arch under consideration forms the bottom part of the façade of the church, which is overhung by a triangular tympanum (not modelled). We study such a structure both in correspondence of the real configuration of the arch, and also in correspondence of modified (virtual) configurations that exhibit additional holes/obstacles within the side abutments. The masonry structure that contains the strut nets as 'thrust lines' (or internal resisting structures) [4] is coloured light brown in the figures that follow. The obstacles are labelled with a number in brackets (in different colours),

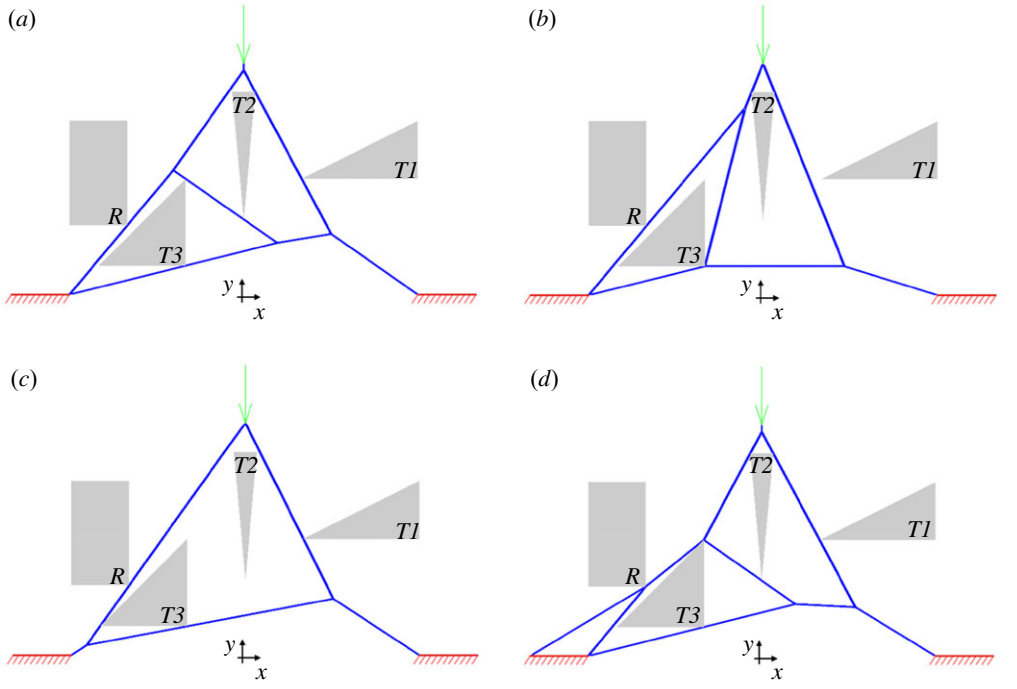

Figure 10. Strut nets resulting from the linear programming problem: a single active vertical force (marked in green) is supported by the shown strut net (blue in colour) with the help of 200 reacting points uniformly spaced along the lengths of the two supporting segments marked in red (100 points for each segment). The net must avoid four regions (marked in grey). The strut net in (*a*) minimizes the total weight of the structure, while those in (*b–d*) minimize the heights of the cleaving planes of the obstacles *T*1, *T*2 and *T*3 at their centres of mass, respectively.

placed at their centres of mass. All the strut nets of the examples presented hereafter have been obtained through the linear programming algorithm of §4, by minimizing the total weight of the structure. Such strut nets lie within the masonry, which implies that the analysed structures are stable under the examined loading conditions, according to the no-tension limit analysis approach by Heyman [4]. The first example illustrated in figure 11 considers the action of a uniformly distributed vertical load q acting on top of the arch, which is lumped in correspondence of 21 points of a discretized version of the boundary of the arch (all the dimensions shown in figure 11 are measured in metres). The load q corresponds to the self-weight of the structure, and has been set equal to 123.79 kN m^{-1} following [27]. The arch stands above a central opening (in grey: obstacle (1) in figure 11) and is constrained with two supporting segments formed by three points each at the bases of the side abutments. Figure 11 shows in blue the feasible strut net composed of two arched structures and a collection of vertical and diagonal struts, which has been obtained through the algorithm of §4.

As a second example, we study a modified (virtual) configuration of the triumphal arch of the San Ippolisto Martire church that exhibits an elliptical portal on top of the right abutment (figure 12). Such an 'obstacle' exhibits horizontal major axis equal to 1.20 m and vertical minor axis equal to 0.60 m. It was approximated by a 22-sided polygon. The structure under consideration is studied by augmenting the same vertical forces analysed in the previous example with horizontal forces obtained by lumping a uniform horizontal load distribution p in correspondence to 20 vertices of a discretized version of the right side of the right abutment. The points where p has been lumped consist of 15 equally spaced points placed along the vertical side of the right side of the right abutment, and six equally spaced points placed along the oblique part of the same right side. We set $p = 0.1q$, since such a loading condition was shown to be safe (without the elliptical

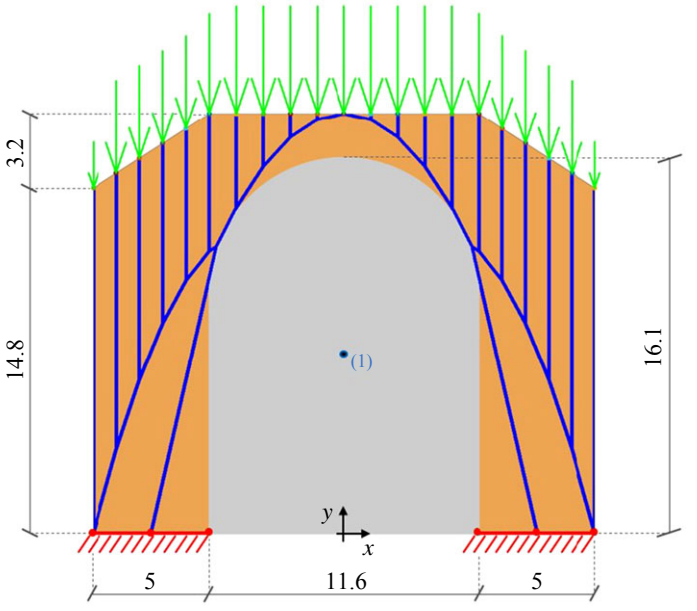

Figure 11. The triumphal arch of a basilica church featuring a central opening modelled as an obstacle (represented in grey; dimensions in metres). The arch support 21 vertical forces acting downwards on the top (in green), which have been obtained by lumping a uniform vertical load acting on top of the arch in correspondence of six equally spaced points placed along the top-oblique segments of the boundary of the structure, and 10 equally spaced points placed in correspondence of the top-horizontal segment of such a boundary. Two supporting segments (in red) have been inserted at the bases of the side abutments. Such segments have been discretized into three potential reactive points, denoted by red spots in the figure. More reactive points could easily be added but three suffice and adding more makes the strut need more sensitive to variations in the applied forces. The half disk on top of obstacle (1) has been approximated by a 98-sided polygon. The feasible strut net marked in blue, which has been obtained through our linear programming formulation, is supported by only two active reaction points within each abutment.

porthole) in the finite-element study presented in [27]. The arch is supported in correspondence of four equally spaced points placed at the bases of the side abutments. It is seen that the feasible strut net shown in figure 12 exhibits four arches and a collection of vertical and diagonal struts.

The final example shown in figure 13 is obtained by 'perturbing' the configuration in figure 12 through the introduction of a walkway at the base of the left abutment (refer to figure 13 for a detailed description of this 'obstacle'). Upon considering the same loading condition of the previous example, the linear programming algorithm of §4 returns a feasible strut net that is again formed by four arched structures and a collection of vertical and diagonal struts, as in the example illustrated in figure 12. The feasible strut net is supported only at extremities of the left abutment in the present case, so as to avoid obstacles (2) and (3).

6. Conclusion

Given a two-dimensional set of forces at the vertices of a convex polygon, some of which are prescribed forces and the remainder reactive forces, our main goal was to determine if a strut net exists avoiding a given set of obstacles, and if so, to construct one such strut net. By approximating each obstacle by a convex polygon, possibly with many sides, we successfully devised an algorithm for doing this. It reduced to a linear programming procedure and was based on finding a suitable concave polyhedral Airy stress function associated with the strut net when all struts are under compression. Additionally, under the assumption that there is just one obstacle, we devised an algorithm for generating regions that provide the maximum amount of

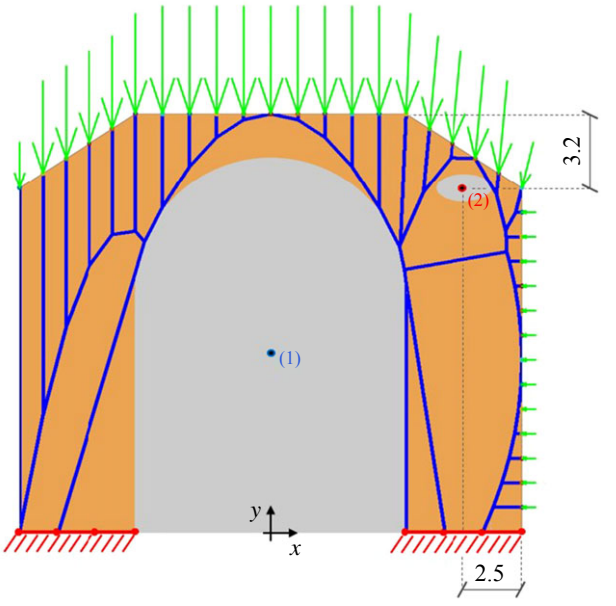

Figure 12. Modified configuration of the arch studied in figure 11, obtained adding an elliptical porthole on top of the right abutment (dimensions in metres), approximated by a 22-sided polygon. Such a configuration is analysed under the combined action of vertical forces acting on top of the arch and horizontal forces acting in correspondence of the side boundary of the right abutment. The resultant of the horizontal forces is set equal to 1/10 of the resultant of the vertical forces [27]. For simplicity, four equally spaced (potential) restraint points have been placed at the bases of the side abutments. The feasible strut net in blue is formed by three arched structures connected to vertical and diagonal struts.

space available to the obstacle, as shown in figure 9 and electronic supplementary material, movie S3. By this we mean that the region available to the obstacle cannot be enlarged in the sense of definitions 3.2 and 3.1. We also obtained partial results (theorem 2.2) in the case where there are q forces strictly inside the convex hull of all points where forces are applied. We established that a strut net supporting these forces, while avoiding p obstacles, p_0 of which intersect this convex hull, can be replaced by a strut net, supporting the same forces and avoiding the same obstacles, that has at most $q + p - p_0$ elementary loops. In figure 6 and electronic supplementary material, movie S1, $q = 0$, and $p = p_0 = 1$ and the number of loops can be reduced until one obtains a final structure that is an open strut net. In figure 8 and electronic supplementary material, movie S2, instead, $q = p = 1$, and $p_0 = 0$, and the final net presents two elementary loops. Our work can be used to determine if a given masonry structure (modelled as an incompressible, no-tension body [4]) can support, under compression, one or more families of given forces (and convex combinations of them). For example, the masonry arch coloured light brown in figures 11–13 can support different families of vertical and horizontal forces (and convex combinations of them), while avoiding various rectangular, semicircular and elliptical obstacles. Alternatively, we may use the strut nets that support the desired families of forces to efficiently design the masonry structures themselves, eliminating unnecessary regions. Constraints on the boundary of the masonry structure can be imposed by introducing appropriate obstacles such as, for instance, those in figures 11–13. Our analysis also applies to structures built from unreinforced concrete since it supports compression but not tension. It can be easily generalized to the problem of finding cable webs under tension that avoid given obstacles and support prescribed nodal forces [13,14].

We address the following generalization of the present study in future work: given a force set $\mathbf{t} = (\mathbf{t}_1, \mathbf{t}_2, \ldots, \mathbf{t}_n)$ and a vector set $\mathbf{f} = (\mathbf{f}_1, \mathbf{f}_2, \ldots, \mathbf{f}_n)$, determine the extreme values of λ such that a strut net avoiding the obstacles supports both $\mathbf{t}$ and $\mathbf{t} + \lambda\mathbf{f}$. Here $\mathbf{f}$ could represent an additional forcing, say, e.g. due to an earthquake [7,30].

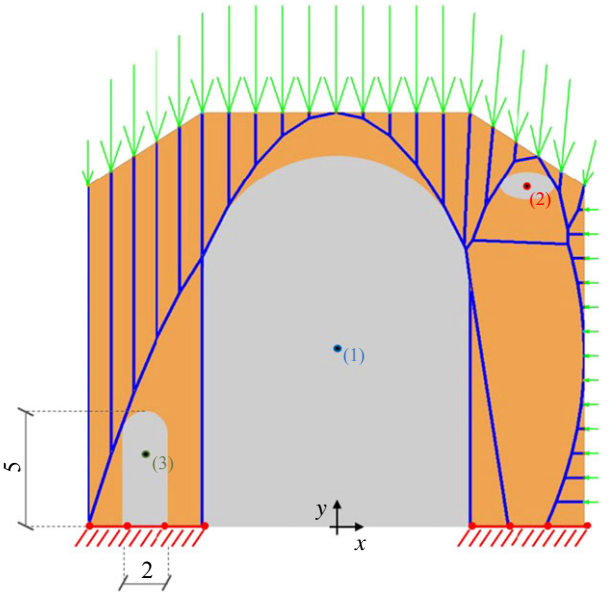

Figure 13. Perturbed configuration of the arch studied in figure 12, obtained by adding a walkway at the base of the left abutment (obstacle 3, dimensions in metres). Such an opening is formed by a rectangular region with 2 m width and 4 m height, which is overhung by an arch with 1 m radius. The latter is approximated with a 22-sided polygon. The present configuration is analysed under the same loading condition of the example in figure 12, and in the presence of an equal number and distribution of (potential) reaction points at the base of the abutments. The feasible strut net in blue is again formed by four arched structures connected to vertical and diagonal struts, as in the example in figure 12. In the present case, however, such a strut net shows only two active reaction points at the bottom of the left abutment.

There are many other avenues that have not been explored in the present paper. An extension of the results to three dimensions would obviously be important, but perhaps very difficult. The stress does have a matrix valued function, the Beltrami stress function, that is analogous to the two-dimensional Airy stress function. However, it is difficult to interpret the constraints on the Beltrami stress function imposed by a negative semidefinite stress field. Another extension is to find a way of generating strut nets supporting q forces strictly inside the convex hull of all points where forces are applied, while avoiding p obstacles, without assuming one starts with a strut net achieving these goals. Further goals are outlined in [31]. One, with or without obstacles, is to allow for some elasticity in the struts, and to determine the possible sets of displacements $\mathbf{u}_1, \mathbf{u}_2, \ldots, \mathbf{u}_n$ at the vertices $\mathbf{x}_1, \mathbf{x}_2, \ldots, \mathbf{x}_n$ when a force set $\mathbf{f}_1, \mathbf{f}_2, \ldots, \mathbf{f}_n$ is applied. (Assuming the force set is such that at least one strut net supporting the forces, yet avoiding any obstacles, exists.) Another is to allow for finite deformations, with or without obstacles. That is, given moving points $\mathbf{x}_1(t), \mathbf{x}_2(t), \ldots, \mathbf{x}_n(t)$ and balanced forces $\mathbf{f}_1(t), \mathbf{f}_2(t), \ldots, \mathbf{f}_n(t)$ that are dependent on time t, when does there exist a single strut net under tension that supports these forces and avoids any obstacles for some given interval of t? Here, single strut net means a strut net wherein the angles between struts change with t but the topology and strut lengths do not; all struts also remain under compression and do not collide. An even more challenging problem results if some of the struts collide as t changes.

Data accessibility. Three movies are provided as electronic supplementary material. Electronic supplementary material, movie S1 illustrates the step-by-step loop reduction procedure for the example depicted in figure 6, whereas electronic supplementary material, movie S2 treats the loop reduction of the strut net represented in figure 8. Finally, electronic supplementary material, movie S3 illustrates the rolling of the cleaving plane to create maximal regions where the obstacle can be placed, as illustrated in figures 9 and 10. The authors confirm that the data supporting the findings of this study are available within the article and its electronic supplementary material [32].

Authors' contributions. A.A.: conceptualization, formal analysis, funding acquisition, investigation, methodology, software, validation, visualization, writing—original draft, writing—review and editing; O.M.: conceptualization, formal analysis, funding acquisition, investigation, methodology, software, validation, writing—original draft, writing—review and editing; G.W.M.: conceptualization, formal analysis, funding acquisition, investigation, methodology, supervision, validation, writing—original draft, writing—review and editing; P.S.: conceptualization, formal analysis, investigation, methodology, software, validation, writing—original draft, writing—review and editing.

All authors gave final approval for publication and agreed to be held accountable for the work performed therein.

Conflict of interest declaration. We declare we have no competing interests.

Funding. O.M. and G.W.M. are grateful to the National Science Foundation for support through Research grants nos. DMS-2008105 and DMS-2107926. AA is grateful to the Italian Ministry of University and Research for support through the PRIN 2017 grant no. 2017J4EAYB.

Acknowledgements. Fernando Fraternali is thanked for suggesting the incorporation of reactive forces and for suggesting many pertinant references.

References

1. Angelillo M, Lourenço PB, Milani G. 2014 Masonry behaviour and modelling. In *Mechanics of masonry structures* (ed. M Angelillo). CISM International Centre for Mechanical Sciences, vol. 551. Vienna, Austria: Springer.
2. Bagi K. 2014 When Heyman's safe theorem of rigid block systems fails: non-Heymanian collapse modes of masonry structures. *Int. J. Solids Struct.* **51**, 2696–2705. (doi:10.1016/j.ijsolstr.2014.03.041)
3. Beatini V, Royer-Carfagni G, Tasora A. 2019 Modeling the shear failure of segmental arches. *Int. J. Solids Struct.* **158**, 21–39. (doi:10.1016/j.ijsolstr.2018.08.023)
4. Heyman J. 1995 *The stone skeleton: structural engineering of masonry architecture*. Cambridge, UK: Cambridge University Press.
5. Alexakis H, Makris N. 2014 Limit equilibrium analysis and the minimum thickness of circular masonry arches to withstand lateral inertial loading. *Arch. Appl. Mech.* **84**, 757–772. (doi:10.1007/s00419-014-0831-4)
6. Alexakis H, Makris N. 2015 Limit equilibrium analysis of masonry arches. *Arch. Appl. Mech.* **85**, 1363–1381. (doi:10.1007/s00419-014-0963-6)
7. Como M. 2017 *Statics of historic masonry constructions*, 3rd edn. Heidelberg, Germany: Springer.
8. Poleni G. 1991 *Memorie istoriche della gran cupola del Tempio Vaticano*. Rome, Italy: Edizioni Kappa. (Anastatic reprint of the original edition of 1748)
9. Jimenez Morales MI. 2002 *Gaudí, la búsqueda de la forma: espacio, geometría, estructura y construcciôn*. Barcelona, Spain: Lunwerg Editores.
10. Huerta S. 2006 Structural design in the work of gaudí. *Archit. Sci. Rev.* **49**, 324–339. (doi:10.3763/asre.2006.4943)
11. Tempesta G, Galassi S. 2019 Safety evaluation of masonry arches. A numerical procedure based on the thrust line closest to the geometrical axis. *Int. J. Mech. Sci.* **155**, 206–221. (doi:10.1016/j.ijmecsci.2019.02.036)
12. Tralli A, Chiozzi A, Grillanda N, Milani G. 2020 Masonry structures in the presence of foundation settlements and unilateral contact problems. *Int. J. Solids Struct.* **191–192**, 187–201. (doi:10.1016/j.ijsolstr.2019.12.005)
13. Bouchitté G, Mattei O, Milton GW, Seppecher P. 2019 On the forces that cable webs under tension can support and how to design cable webs to channel stresses. *Proc. R. Soc. A* **475**, 20180781. (doi:10.1098/rspa.2018.0781)
14. Milton GW. 2017 The set of forces that ideal trusses, or wire webs, under tension can support. *Int. J. Solids Struct.* **128**, 272–281. (doi:10.1016/j.ijsolstr.2017.08.035)
15. O'Dwyer D. 1999 Funicular analysis of masonry vaults. *Comput. Struct.* **73**, 187–197. (doi:10.1016/S0045-7949(98)00279-X)
16. Block P, Ochsendorf J. 2007 Thrust network analysis: a new methodology for three-dimensional equilibrium. *J. Int. Assoc. Shell Spat. Struct.* **48**, 167–173.
17. Marmo F, Rosati L. 2017 Reformulation and extension of the thrust network analysis. *Comput. Struct.* **182**, 104–118. (doi:10.1016/j.compstruc.2016.11.016)
18. Giaquinta M, Giusti E. 1985 Researches on the equilibrium of masonry structures. *Arch. Ration. Mech. Anal.* **88**, 359–392. (doi:10.1007/BF00250872)

19. Del Piero G. 1998 Limit analysis and no-tension materials. *Int. J. Plast.* **14**, 259–271. (doi:10.1016/S0749-6419(97)00055-7)
20. Lucchesi M, Padovani C, Pasquinelli G, Zani N. 2008 *Masonry constructions: mechanical models and numerical applications*, p. 1–168. Lecture Notes in Applied and Computational Mechanics, vol. 31. Berlin, Heidelberg: Springer-Verlag.
21. Fortunato A. 2010 Elastic solutions for masonry-like panels. *J. Elast.* **98**, 87–110. (doi:10.1007/s10659-009-9219-z)
22. De Faveri S, Freddi L, Paroni R. 2013 No-tension bodies: a reinforcement problem. *Eur. J. Mech. A/Solids* **39**, 163–169. (doi:10.1016/j.euromechsol.2012.11.006)
23. Fraternali F. 2010 A thrust network approach to the equilibrium problem of unreinforced masonry vaults via polyhedral stress functions. *Mech. Res. Commun.* **37**, 198–204. (doi:10.1016/j.mechrescom.2009.12.010)
24. Fraternali F, Carpentieri G. 2014 On the correspondence between 2D force networks and polyhedral stress functions. *Int. J. Space Struct.* **29**, 145–159. (doi:10.1260/0266-3511.29.3.145)
25. Pintucchi B, Zani N. 2009 Effects of material and geometric non-linearities on the collapse load of masonry arches. *Eur. J. Mech. A/Solids* **28**, 45–61. (doi:10.1016/j.euromechsol.2008.02.007)
26. Fraternali F, Angelillo M, Fortunato A. 2002 A lumped stress method for plane elastic problems and the discrete–continuum approximation. *Int. J. Solids Struct.* **39**, 6211–6240. (doi:10.1016/S0020-7683(02)00472-9)
27. De Luca A, Giordano A, Mele E. 2004 A simplified procedure for assessing the seismic capacity of masonry arches. *Eng. Struct.* **26**, 1915–1929. (doi:10.1016/j.engstruct.2004.07.003)
28. Skelton RE, Fraternali F, Carpentieri G, Micheletti A. 2014 Minimum mass design of tensegrity bridges with parametric architecture and multiscale complexity. *Mech. Res. Commun.* **58**, 124–132. (doi:10.1016/j.mechrescom.2013.10.017)
29. Zalewski W, Allen E. 1998 *Shaping structures: statics*. New York, NY: John Wiley & Sons.
30. Orduña A. 2017 Non-linear static analysis of rigid block models for structural assessment of ancient masonry constructions. *Int. J. Solids Struct.* **128**, 23–35. (doi:10.1016/j.ijsolstr.2017.07.022)
31. Bouchitté G, Mattei O, Milton GW, Seppecher P. 2020 Guiding stress with cable networks and the spider web problem. *SIAM News*, October 1st.
32. Amendola A, Mattei O, Milton GW, Seppecher P. 2023 The obstacle problem in no-tension structures and cable nets. Figshare. (doi:10.6084/m9.figshare.c.6350216)